

Modelling of Fatigue Failure for Plasma Coated Members Using Artificial Intelligence Technique

Hani. A. AL- Rawashdeh^{1*} A. O. Hasan^{1,2} Kamis issa² Jehad bin yamin³ U Al-Qawabeha⁴
1.Department of Mechanical Engineering, Al-Hussein Bin Talal University, Maan P.O. Box 20, Jordan
2.School of Mechanical Engineering, University of Birmingham, Birmingham B15 2TT, UK
3.Department of Mechanical Engineering, university of Jordan, amman
4.Department of Mechanical Engineering, Tafilah Technical University, Tafilah, Jordan

Abstract

Coating materials in form of powder such as Magnesium Zirconate, Aluminum Bronze and Molybdenum were mixed in different portions and sprayed on steel specimen to find the fatigue properties of steel using plasma technique. The effect of coating mixture on the number of cycles needed for failure under different loads was done experimentally. A cyclic loading was applied to it repeatedly until failure occurs. The results were compared with those for the same specimen without coating. The results were then modelled using Artificial Intelligence Technique then optimized for maximum cycles of coated substance failure. The results showed significant improvement to the specimen's resistance to failure with coating. Further, models were developed out of the experimental data and tested for accuracy and gave satisfactory results. However, the time consumed by the GA method was greater than that consumed by the same software for the ANN model development. Also, sensitivity analysis showed that the key effect for the variables studied was for the load while the least effect was for the Molybdenum mixture. On the other hand, using GA method, the importance of variables was maximum for the load and minimum for Magnesium oxide and Zirconate oxide mixture. Further, using the correlation method, there was strong negative (i.e. inverse relationship) correlation between the number of cycles and load and weak with Magnesium oxide and Zirconate oxide mixture while strong positive correlation was shown with Molybdenum and least positive for Aluminum Copper Balance.

Keywords: Artificial neural network, modeling, Plasma coating, fatigue failure.

Introduction

When the material is subjected to dynamic and fluctuating stresses, the fatigue is one of the failure modes which occurs in its structure, this type of failure occurs after a long period of time during a repeated stress or strain cycling. Fatigue is brittle even in normal ductile metals, so not much of gross plastic deformation associated with failure. One of the most effective methods of increasing fatigue performance is by imposing residual compressive stresses within a thin outer surface layer. a surface tensile stress of external origin will be partially nullified and reduced in magnitude of residual compressive stress, the outcome is that the likelihood of crack formation and there of fatigue failure is reduced. Failure that occurs by the simultaneous action of cyclic stress and chemical attack is termed corrosion fatigue. Corrosive environment have a deleterious influence and produce shorter fatigue life. Crack propagation rate enhanced as a result of the corrosive environment. Several approaches to corrosion fatigue prevention exist. On one hand , measures could be taken to reduce the rate of corrosion by different technique, one of the most technique will be used in our work is plasma surface coating by depositing metallic coating to improve the surface of the substrate.

Plasma spray coating system uses coating material in the form of powder and plasma flame as the source of heat to melt the powder. Flame spraying is the process of depositing fine, molten particles of metals, alloys, ceramics, and cermets of plastics to form a coating. The plasma spray process has the ability to offer a high-temperature and high-velocity environment to the spraying powders, during the process, the powder material may undergo chemical change during the deposition due to excessive heating. o make a choice for deposition process it depends strongly on the expected coating properties for the application and coating deposition cost Gärtner et al (2006). The produced coatings by thermal spraying could have some negative effect on the sample part; for instant the needed contact area between the splat and the substrate which determines the coating properties. The real contact between splats increases from about 20 to 60 % with particle impact velocities, as long as the particles are not either too much superheated or below their melting temperature Racek (2010). Another cause might appear is splashing of the melted particles. During flattening upon impact can significantly affect the coating properties Splats deposited on splashed material exhibit lower adhesion and this effect is more significant when spraying metals because the splashed material is oxidized rather fast due to the small droplet sizes, also substrate geometry may affect the flow of impacting and splashing particles Racek (2010). Many components are subjected to alternating or fluctuating loading cycles during services, and failure by fatigue is fairly common concerns. Murakami and Shimada (2009) have studied the corrosion and marine fouling behaviors of different flame - sprayed coatings.

The aging of TBC's topcoat depends strongly upon the spray conditions and powder morphologies used to

spray or deposit it, conditions acting on its sintering Golosnoy et al (2009), Cipitria et al (2009), Markocsan et al (2009). The second problem is the oxidation of bond coat with the formation of Thermally Grown Oxide (TGO) Feuerstein et al (2008) as well as the bond coat corrosion with oxides such as CMAS (calcium-magnesium-aluminosilicate) Li et al (2010), Vassen et al (2009) or vanadium oxide Chen et al (2009). Feuerstein et al (2008) have shown that the most advanced thermal barrier coating (TBC) systems for the hot section components (combustors, blades and vanes) of aircraft engines and power generation systems, consist of EBPVD-applied (Electron Beam Physical Vapor Deposition) yttria-stabilized zirconia coating and platinum modified diffusion aluminide bond coating. The aim of this experimental work is to study the fatigue limit of the coated material and distinguish the best-coated combination of the sprayed powder, Artificial Neural Networks needed to predict the mechanical properties of the coated material.

Experimental work

Self – bonding stainless composite powder was used as percolating for bonding purposes. Samples surfaces should be decreased and all surface oxidation have to be removed by grit blasting. Base substrate of samples has been roughed by a grit blasting as preparation before using coating powders by plasma technique.

METCO 7M Plasma Flame Spray System was used in experimental work, hydrogen was used to avoid any Oxygen and water vapor. Pre-purified Hydrogen and Argon was carried out to get smoothly process. The gas required flow and pressure as seen in Table (1) below:

Table (1): Flow pressure data

Gas	Required flow	Required pressure (kPa)
Argon	224 SCFH	689.45
Hydrogen	30 SCFH	517

The gun setup is done by installing the suitable nozzle and setting the coating angle, the nozzle size is easily selected from the manufacture manual with respect to the particle size powder, while the angle of coating is chosen to be 90 degree. Table (2) below shows the plasma spray coating operational parameters as recommended by the manufactures for these specified powder:

Table (2): Plasma spray coating operational parameters

Wheel speed (rpm)	Nozzle	Plasma Gas flow (gs ⁻¹)		Current DC (A)	Voltage DC (V)	Spray distance (mm)	Spray rate (gs ⁻¹)
		A2	H2				
15	GH	10.08	1.89	500	70	76-127	0.535

The heat for spraying is produced by a high-intensity electric arc confined within the spray gun. The arc operates on direct current from a rectifier-type of powder supply unit feed from alternating current mains. The final coatings and loads used in this experimental work are summarized in Table (3) below.

With each sample subjected to various loads during tests ranging from 120 to 240 N at a 30 N increment.

Table (3): Specifications of the coatings used

Group	M1 %	M2 %	M3 %	Density
A	90	5	5	4.56
B	90	0	10	4.77
C	90	10	0	4.54
D	85	10	5	4.77
E	85	5	10	4.89
F	0	0	100	9
G	0	100	0	6.7
H	100	0	0	4.3
X	0	0	0	0

M1 - Magnesium oxide 24%/ Zirconate oxide 76%, M2 - Aluminum 10% Copper Balance
 M3 - Molybdenum 99 %, X Uncoated sample.

Artificial Neural Networks

The lack of progress in predicting mechanical properties is because of their dependence on large numbers of variables. Nevertheless, there are clear patterns, which experienced metallurgists recognize, and understand. Neural network models are extremely useful in such circumstances, not only in the study of mechanical properties but wherever the complexity of the problem is overwhelming from a fundamental perspective and where simplification is unacceptable.

General method of regression which avoids these difficulties is neural network analysis, illustrated at first using the familiar linear regression method. A network representation of linear regression is illustrated in Fig. 1a. The inputs xi (concentrations of coating) define the input nodes, the number of cycles to reach failure represents

the output node. Each input is multiplied by a random weight w_i and the products are summed together with a constant b (bias) to give the output

$$NET_i = \sum_{j=1}^n w_{ij}x_j + b_i \quad (1)$$

The summation is an operation which is hidden at the hidden node. Since the weights and the constant b were chosen at random, the value of the output will not match with experimental data. The weights are systematically changed until a best-fit description of the output is obtained as a function of the inputs; this operation is known as training the network.

The activation function provides a curvilinear match between the input and output layers. In addition, it determines the output of the cell by processing the net input to the cell. The selection of an appropriate activation function significantly affects network performance. There are many ways to define the activation function, such as the threshold function, step activation function, sigmoid function, and hyperbolic tangent function. The type of activation function depends on the type of neural network to be designed. A sigmoid function is widely used for the transfer function. Logistic transfer function of the ANN model in this study is given in the equation (2) below (for logistic activation function as an example):

$$f(NET_i) = \frac{1}{1+e^{-NET_i}} \quad (2)$$

In the output layer, the output of network is produced by processing data from hidden layer and sent to external world. The significant advantages of artificial neural networks are learning ability and the use of different learning algorithms. The most important factor which determines its success in practice, after the selection of ANN architecture, is the learning algorithm. In order to obtain the output values closest to the numerical values, the best learning algorithm and the number of optimum neurons in the hidden layer must be determined. After that, sensitivity analysis using this ANN model was used to recognize the major and minor contributors to the job oil yield from input variables.

Sensitivity Analysis using ANN model can rank and select the major and input variables through its analysis. Sensitivity analysis with partial differential is based on calculation of input, weights and output variables from the ANN simulation model. The calculation of sensitivity (S) is as follows:

$$S = \frac{\partial O}{\partial I} = \hat{O} \sum_{j=1}^J (w_{ij}^1 \hat{H} w_{ij}^2) \quad (3)$$

$$S = \frac{\partial f(O)}{\partial x} \sum_{j=1}^J \left(w_{ij}^1 \frac{\partial f(H)}{\partial x} w_{ij}^2 \right) \quad (4)$$

Where O is output and H is a hidden node that have to be differentiated, w_{ij}^1 and w_{ij}^2 are the weights with respect to the first and second connection of hidden layer.

The first connection is for input and hidden layer and the second connection is for hidden node and output layer. It computes each set of input and output data. If the network has bias, the equation becomes:

$$S = \hat{O} \sum_{j=1}^J \left((w_{ij}^1 H' + b_{ij}^1) w_{ij}^2 + b_{ij}^2 \right) \quad (5)$$

$$S = \frac{\partial f(O)}{\partial x} \sum_{j=1}^J \left(\left(w_{ij}^1 \frac{\partial f(H)}{\partial x} + b_{ij}^1 \right) w_{ij}^2 + b_{ij}^2 \right) \quad (6)$$

By using Equation 6, the value for each input corresponding to a single and multiple outputs can be obtained. All ANN models for sensitivity analysis use the training data to perform sensitivity value. By referring to sensitivity value, the input variables can be ranked for their contribution to the output. The results with higher values represent major factors and those with lower values represent minor factor.

The structure of the network used in this study is shown in Figure (1) below. It consists of 5 variables in the input layer i.e. load, M1, M2, M3 and density, with one output i.e. the number of cycles at failure.

The activation function for both hidden and output layers was chosen to be the sigmoid function as shown in equation (2).

For the Genetic programming, a software called GPdotNET developed by Dr Bahrudin (2015) was used for both modelling and optimization.

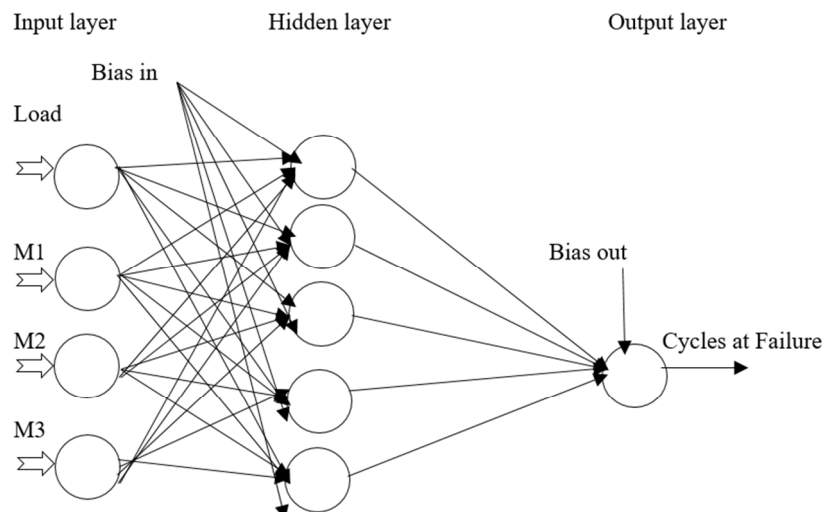


Figure (1): Artificial Neural Network Design

Results and discussion

Variable Importance and Sensitivity Analysis

An importance and sensitivity tests were performed using both GA and ANN approaches respectively, to find the influence of the parameters on the final results. They are summarized in Table (4) below.

The importance of each variable is computed by randomizing its input values and then computing the decrease in the R-square between model outputs and actual values. The results for all variables are then normalized so that they add up to 1. Sensitivity analysis generally refers to the assessment of the importance of predictors in the respective (fitted) models. In short, given a fitted model with certain model parameters for each predictor, what the effect would be of varying the parameters of the model (for each variable) on the overall model fit. The results show that the number of cycles needed for failure is most sensitive to the load applied while it is least sensitive to the mixture M3 of the coating.

Table (4): Variable importance / sensitivity

Method \ Variable	Load	M1	M2	M3
Importance (GA Method)	0.52	0.060345	0.2076	0.2121
Sensitivity (ANN Method)	7.362025	3.180290	1.926656	1.607934

On the correlation level, there is good inverse relationship between the load and cycles at failure and very weak one with M1 mixture. On the positive side, density has the greatest linear relationship (though weak in effect) with cycles at failure. Having an overall view on the data, a correlation analysis was done using MS Excel and the results are summarized in Table (5) below.

Table (5): Summary of correlation analysis

	Load	M1	M2	M3	Cycles at failure
Load	1				
M1	0	1			
M2	-3.9E-18	-0.44231	1		
M3	-3.9E-18	-0.44231	-0.20936	1	
Density	0	-0.13153	0.296949	0.677817	
Cycles at failure	-0.64641	-0.15684	0.196772	0.245464	1

Mathematical modelling and optimization

The regression models predicted by both ANN and GA methods are shown and discussed here. First, the weights and biases given by the ANN method are summarized in Tables (6 and 7) respectively.

As for the ANN method, a network was built which has the configuration 4-7-1 i.e. with 7 neurons in the hidden layer using Tanh and Exponential activation functions for the input and output hidden layers respectively. These functions were chosen after testing all possible combinations between several functions e.g. logistic, linear, sin and others. This combination gave the least error and converged in the least amount of computational time. A summary of the network configuration and performance is shown in Table (6).

Table (6): Summary of the ANN model performance

Network Name	Training Performance	Testing Performance	Validation Performance	Training Algorithm	Input Activation	Output Activation	Error Function
MLP 4-7-1	0.99925207	0.999654	0.999699	SOS	Tanh	Exponential	BFGS 119

The variation of the amount of errors with iteration is shown in Figure (2) below.

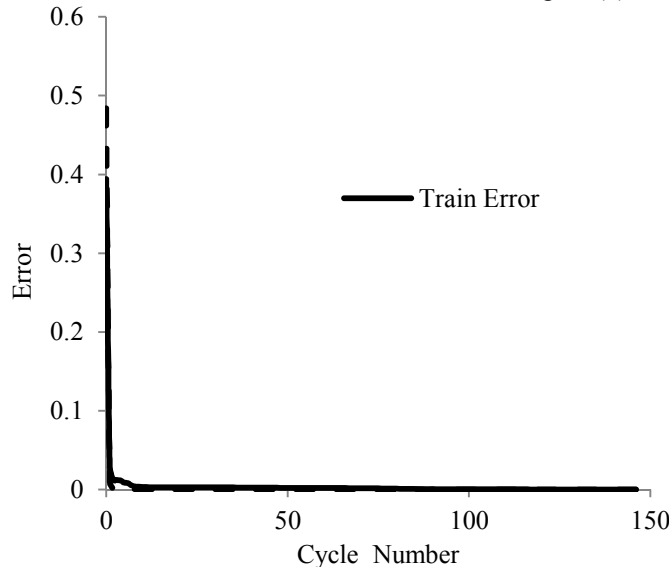


Figure (2): Variation of error during modelling progress

The results of the ANN model in terms of the weights given to each neuron as well as the bias for both inputs and output is summarized in Tables (7 and 8).

Table (7): Weights for the input hidden layer

to the input layer	bias	Load	M1	M2	M3
1st neuron	-0.09775	1.60121	3.93113	-0.18767	-10.88368
2nd neuron	-2.00056	-0.98566	1.49227	9.62920	5.87242
3rd neuron	-0.71559	-2.61767	-2.70278	1.30373	6.33915
4th neuron	-6.93321	0.23434	8.58513	-2.80235	0.48720
5th neuron	3.10961	1.83620	1.03516	2.17651	-0.83864
6th neuron	1.91113	0.53504	0.22114	2.14651	-0.17097
7th neuron	-2.22469	-1.70705	0.83419	3.15919	2.62470

Table (8): Weights for the output layer

output layer	bias	1st neuron	2nd neuron	3rd neuron	4th neuron	5th neuron	6th neuron	7th neuron
output	-2.64569	-2.31630	5.10635	-1.15689	5.87685	1.08130	0.21402	2.62357

Using equations (1 and 2) with modifications as per the activation functions used one can derive the regression equation for this model. However, it will be too lengthy to write. An example of the formula is shown in equations (7) below:

$$\left. \begin{aligned} \text{NET}_1 &= (1.60121 * \text{Load} + 3.93113 * \text{M1} - 0.18767 * \text{M2} - 10.88368 * \text{M3}) - 0.09775 \\ \text{NET}_2 &= (-0.98566 * \text{Load} + 1.49227 * \text{M1} + 9.62920 * \text{M2} + 5.87242 * \text{M3}) + 2.00056 \\ \text{NET}_3 &= (-2.61767 * \text{Load} - 2.70278 * \text{M1} + 1.30373 * \text{M2} + 6.33915 * \text{M3}) - 0.71559 \end{aligned} \right\} \quad (7)$$

As for the Hyperbolic Tangent (Tanh) activation function, it can be written as in equation (8)

$$\text{Tanh}(\text{NET}_i) = \frac{e^{\text{NET}_i} - e^{-\text{NET}_i}}{e^{\text{NET}_i} + e^{-\text{NET}_i}} \quad (8)$$

hence, the values of NET_i are substituted in the equation.

The output layer has Exponential activation function e^{-x} . Hence the final equation can be written as:

$$Y = e^{-(-2.3163 * \text{Tanh}(\text{NET}_1) + 5.10635 * \text{Tanh}(\text{NET}_2) - 1.15689 * \text{Tanh}(\text{NET}_3) + 5.87685 * \text{Tanh}(\text{NET}_4) + 1.0813 * \text{Tanh}(\text{NET}_5) + 0.21402 * \text{Tanh}(\text{NET}_6) + 2.62357 * \text{Tanh}(\text{NET}_7)) - 2.3163} \quad (9)$$

Finally, the value of the output must be de-normalized to get the number of cycles' value.

A comparison between the outputs of the model compared with the experimental data is shown in Figure (3) below. The figure shows good accuracy of the model compared with the experimental data.

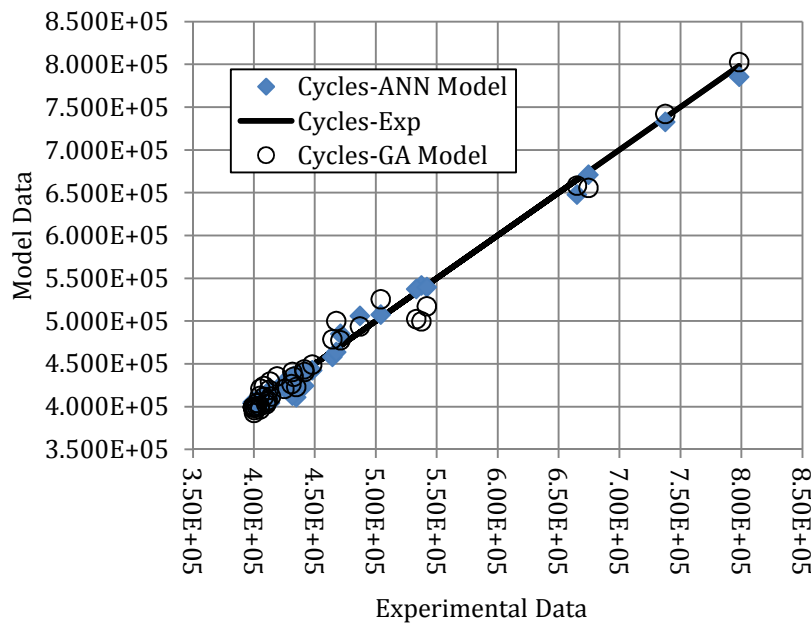


Figure (3): ANN and GA models comparison

As for the Genetic Algorithm, the final results are shown usually in the form of a Genetic Chart shown below in Figure (4).



Figure (4): Genetic Algorithm map

This figure can be rewritten in equation form as shown in equation (10) below.

$$Y = \frac{(((R6 + ((R6 - X4) + X1)) - ((X3 * (R1/R4) + (R3 + (X2 + R5)))))) + (((X2 - X2) - (X3 * R1))/X3) + (((R1/R1) - R5) - X4))}{(((R1 * X1) * (X1 * R6)) - (X4 + X4)) * (((X4 - R4) - X2) * ((R4 - X3) + R6)) - (((R6 + R2) + (X1/X4)) + (((X3 * R3) * (X4 * R6)) * ((R2/X2) * (R2 * R6))))} \quad (10)$$

Where Y = cycles at failure, X1 = Load, X2 = M1, X3 = M2, X4 = M3,
 R1 = 3.9325, R2 = 2.4961, R3 = 9.5953, R4 = 1.3848, R5 = 3.1761 and R6 = 6.518

The performance of this model is shown in Figure (3) along with that for the ANN for comparison. The model predicted the experimental data with good accuracy too. But, compared with that for ANN, the GA model was slightly less accurate with more time needed for computations.

Conclusions

- 1- Sensitivity analysis showed strong dependence of the failure on the load and M3 and least to M1 and M2 mixtures.
- 2- Correlation analysis showed inverse effect of failure to increasing the load.
- 3- Mathematical models were developed to study the effect of each coating mixture on failure behavior.
- 4- The models built using the ANN technique were more accurate and less time consuming.

Acknowledgement

The author would like to extend a vote of thanks to Dr Bahrudin I. Hrnjica for allowing me to use his software GPdotNET for both ANN and GA analysis.

References

Cipitria A., I.O. Golosnoy, T.W. Clyne, (2009) A sintering model for plasma-sprayed zirconia TBCs. Part I: Free-standing coatings, *Acta Materialia* 57 980–992
 Chen Z., J. Mabon, J.-G. Wen, R. Trice, (2009) Degradation of plasma-sprayed yttrium-stabilized zirconia coatings via ingress of vanadium oxide, *Journal of the European Ceramic Society* 29 1647–1656
 Davis J. R. (ed.) (2004) *Handbook of Thermal Spray Technology* (pub.) ASM Int. Materials Park OH, USA.
 Feuerstein A., J. Knapp, T. Taylor, A. Ashary, A. Bolcavage, and N. Hitchman, (2008) *Technical and Economical Aspects of Current Thermal Barrier Coating Systems for Gas Turbine Engines by Thermal*

- Spray and EBPVD: A Review, *Journal of Thermal Spray Technology* 17(2) 199-213
- Gärtner F., T. Stoltenhoff, T. Schmidt, and H. Kreye, (2006) The Cold Spray Process and Its Potential for Industrial Applications, *Journal of Thermal Spray Technology*, 15(2) 223-232
- Golosnoy I.O., A. Cipitria, and T.W. Clyne, (2009) Heat Transfer Through Plasma-Sprayed Thermal Barrier Coatings in Gas Turbines: A Review of Recent Work, *Journal of Thermal Spray Technology* 18(5-6) 809-821
- Li L., N. Hitchman, and J. Knapp, (2010) Failure of Thermal Barrier Coatings Subjected to CMAS Attack, *Journal of Thermal Spray Technology* 19(1-2) 148-155
- Markocsan N., P. Nylén, J. Wigren, X.-H. Li, and A. Tricoire, (2009) Effect of Thermal Aging on Microstructure and Functional Properties of Zirconia-Base Thermal Barrier Coatings, *Journal of Thermal Spray Technology* 18(2) 201-208
- Murakami K. and M. Shimada, (2009) Development of Thermal Spray Coatings with Corrosion Protection and Antifouling Properties, in *Thermal Spray 2009: Proceedings of the International Thermal Spray Conference* (eds.) B.R. Marple, M.M. Hyland, Y.-C. Lau, C.-J. Li, R.S. Lima, G. Montavon (pub.) ASM Int. Materials Park, OH, USA 1041-1044
- Racek O., (2010) The Effect of HVOF Particle-Substrate Interactions on Local Variations in the Coating Microstructure and the Corrosion Resistance, *Journal of Thermal Spray Technology* 19(5) 841-851
- Vassen R., A. Stuke, and D. Stöver, (2009) Recent Developments in the Field of Thermal Barrier Coatings, *Journal of Thermal Spray Technology* 18(2) 181-186
- Vuoristo P. and P. Nylen, (2007) Industrial and Research Activities in Thermal Spray Technology in the Nordic Region of Europe *Journal of Thermal Spray Technology* 16(4) 466-471
- Zhang J., Z. Wang, P. Lin, W. Lu, Z. Zhou, and S. Jiang, (2011) Effect of Sealing Treatment on Corrosion Resistance of Plasma-Sprayed NiCrAl/Cr₂O₃-8 wt.%TiO₂ Coating, *Journal of Thermal Spray Technology* 20(3) 508-513
- Bahrudin I. Hrnjica, *GPdotNET V4.0 – artificial intelligence tool [Computer program]*, <http://gpdotnet.codeplex.com>, accessed {1-6-2015}.